Published in final edited form as:
J Surg Res. 2011 July ; 169(1): e27–e36. doi:10.1016/j.jss.2011.01.043.

PEPTIDE INHIBITORS OF MK2 SHOW PROMISE FOR INHIBITION OF ABDOMINAL ADHESIONS

Brian C. Ward, Ph.D.[1], **Sandra Kavalukas**[2], **Jamie Brugnano**[1], **Adrian Barbul, M.D.**[2], and **Alyssa Panitch, Ph.D.**[1]

[1]Weldon School of Biomedical Engineering, Purdue University, West Lafayette, IN 47907 USA

[2]Sinai Hospital of Baltimore / Johns Hopkins Medical Institutions, Baltimore, MD 21215 USA

Abstract

Background—Abdominal adhesions are a common side effect of surgical procedures with complications including infertility, chronic pain, and bowel obstruction, which may lead to the need for surgical lyses of the adhesions. Mitogen-activated protein kinase-activated protein kinase 2 (MK2) has been implicated in several diseases involving inflammation and fibrosis. Thus, the development of a cell-penetrating peptide (CPP) that modulates MK2 activity may confer therapeutic benefit after abdominal surgery in general and more specifically after bowel anastomosis.

Study Design—This study evaluated the function of a CPP inhibitor of MK2 in human mesothelial cells and in a rat bowel anastomosis model. To determine IC50 and basic specificity, kinase inhibition was performed using a radiometric assay. Enzyme-Linked Immunoassay (ELISA) was used to evaluate interleukin-6 (IL-6) expression in response to IL-1β and tumor necrosis factor-α (TNF-α) stimulation *in vitro* to validate MK2 kinase inhibition. Following bowel anastomosis (10 rats for each control and treatment at 4 and 10 days), the rats were evaluated for weight loss, normal healing (colonic burst strength and hydroxyproline content at the anastomosis), and number and density of adhesions.

Results—The IC50 of the MK2 inhibitor peptide (22μM) was similar to that of the nonspecific small molecule Rottlerin (IC50=5μM). The MK2 inhibitor peptide was effective at suppressing IL-1β and TNF-α stimulated IL-6 expression in mesothelial cells. *In vivo*, the MK2 inhibitor peptide was effective as suppressing both the density and number of adhesions formed as a result of bowel anastomosis. Importantly, the peptide had no negative effect on normal healing.

Conclusions—In conclusion, the peptide inhibitor of MK2, MMI-0100, has the potential to significantly reduce inflammation through suppression of inflammatory cytokine expression and showed promise as a therapeutic for abdominal adhesions.

Address correspondence to: Alyssa Panitch, PhD, 206 South Martin Jischke Drive, West Lafayette, IN 47907-2032. Tel: 765-496-1313; Fax: 765-496-1459; apanitch@purdue.edu.

Declaration of Interest

A. Panitch has a financial conflict of interest. Moerae Matrix, Inc has a license to the technology described in the manuscript, and A. Panitch owns greater than a 5% interest in the company.

Keywords

IL-1β; IL-6; MapKap Kinase 2; MK2; TNF-α; abdominal adhesion

Introduction

Abdominal adhesions are a common side effect of surgical procedures, with up to 93% of all abdominal surgeries resulting in adhesions [1,2]. Associated complications that include infertility, chronic pain, and bowel obstruction may require secondary (adhesiolysis) surgeries to remove the adhesions [3]. In 2004, approximately 305,000 surgical procedures were performed to treat intestinal obstructions [4] and survey data suggest that approximately 180,000 of those procedures were attributable to abdominal adhesions [1]. Considering that obstruction-associated complications may include death, together with the absence of current treatment options that reduce risk of adhesion formation in bowel anastomosis procedures, new therapies are greatly needed.

Mesothelial cells lining the surface of the peritoneal cavity play a role in normal healing as well as in the formation of surgical adhesions. Mesothelial cells can produce IL-6, and IL-6 expression has been correlated with adhesion formation. Agents suppressing IL-6 expression have therapeutic potential for reducing adhesions as well as for other human inflammatory disorders in which IL-6 has been implicated. These include not only abdominal and peritoneal adhesions [5–10], but also rheumatoid arthritis and other arthritides [11,12], acute CNS infection [13], multiple myeloma [14], renal cell carcinoma [15], bronchial asthma [16], breast cancer [17], Castleman's disease [5], cardiac myxoma [18], and ovarian cancer [19–22]. Thus, a peptide-based inhibitor of IL-6 expression might have significant impact on human disease in general and specifically in reducing adhesion formation.

Due to the role inflammation plays in adhesion formation, we designed a peptide inhibitor (MMI-0100) to mitogen-activated protein kinase-activated protein kinase 2 (MK2). MK2 is known to play a major role in several inflammatory and fibrotic disorders [12,23–30], via upregulation of inflammatory cytokines subsequent to MK2 activation. The relationship between MK2 activity and IL-6 expression has been elucidated primarily through studies employing MK2 knockout mice, cells obtained from MK2 knockout mice, or cells where MK2 has been suppressed by dsRNA. Many of these studies provide strong support that activated MK2 enhances stability of IL-6 mRNA through phosphorylation of proteins interacting with the AU-rich 3' untranslated region of IL-6 mRNA [12,30–33]. Specifically, Rousseau *et al*. showed that MK2 is principally responsible for phosphorylation of heterogeneous nuclear ribonucleoprotein A0 (hnRNPA0), an RNA-binding protein that stabilizes IL-6 mRNA [34]. Several additional studies investigating diverse inflammatory diseases have directly correlated IL-6 expression with MK2 activation [12,30,31,33]. Thus, suppression of IL-6 expression and hnRNPA0 phosphorylation were utilized in our investigation as measures of MK2 inhibition.

Hayess and Benndorf described a peptide inhibitor of MK2 that was derived from the heat shock protein beta-1 (HSPB1) consensus sequence KKKALNRQLGVAA [35]. While this peptide does inhibit MK2 activity *in vitro*, it lacks a cell-penetrating peptide (CPP) that facilitates entry into cells. We previously demonstrated that a cell-penetrating derivative of the Hayess and Benndorf peptide, WLRRIKAWLRRIKALNRQLGVAA, inhibited HSPB1 phosphorylation in human keloid fibroblasts [36]. While demonstrating functional activity [36], additional work with this peptide indicated that the CPP sequence itself dramatically decreased the kinase specificity of the peptide and also increased its associated toxicity [37]. Thus, the cell-penetrating MK2 inhibitor peptide employed in this study, MMI-0100,

contains the CPP YARAAARQARA, which both maximizes peptide specificity and minimizes toxicity [38].

We investigated whether MMI-0100 would suppress expression of the pro-inflammatory cytokine IL-6 and inhibit hnRNPA0 phosphorylation. Further, we investigated whether a single dose of the MK2 inhibitor peptide, locally delivered at the time of bowel anastomosis surgery, would significantly inhibit adhesion formation without impairing normal healing. The data presented suggest that MMI-0100 holds promise as a potential therapy to reduce adhesion formation in conjunction with general abdominal surgery and, more specifically, in bowel anastomosis procedures.

Materials and Methods

Peptide synthesis and purification

Peptides were synthesized on Rink-amide or Knorr-amide resin (Synbiosci Corp. Livermore, CA) using standard FMOC chemistry [39] on a Symphony® Peptide Synthesizer (Protein Technologies, Inc., Tucson, AZ). The coupling reagent for the amino acids (Synbiosci Corp.) was 2-(1H-Benzotriazole-1-yl)-1,1,3,3-tetramethylaminium hexafluorophosphate/N-methylmorpholine (HBTU/NMM) (Anaspec, – Freemont, CA /Sigma, St. Louis, MO). Following synthesis, the peptide was cleaved from the resin with a trifluoroacetic acid-based cocktail (95% trifluoroacetic acid, 2.5% water, 1.25% triisopropylsilane, and 1.25% ethanedithiol), precipitated in ether, and recovered by centrifugation. The recovered peptide was dried *in vacuo*, resuspended in MilliQ purified water, and purified using an FPLC (ÄKTA Explorer, GE Healthcare, Piscataway, NJ) equipped with a 22/250 C18 prep-scale column (Grace Davidson, Columbia, MD). An acetonitrile gradient with a constant concentration of either 0.1% trifluoroacetic acid or 0.1% acetic acid was used to achieve purification. Desired molecular weight was confirmed by time-of-flight MALDI mass spectrometry using a 4800 *Plus* MALDI TOF/TOF™ Analyzer (Applied Biosystems, Foster City, CA).

Radiometric IC_{50} determination

IC_{50} value for the MK2 inhibitor peptide was determined using Millipore's IC_{50}*Profiler* Express service. The IC_{50} value was estimated from a 10-point curve of one-half log dilutions. Peptide was supplied in DMSO. Specifically, human recombinant MK2 (h) (5–10mU) was incubated with 50 mM sodium β-glycerophosphate (pH = 7.5), 0.1 mM EGTA, 30 μM of substrate peptide (KKLNRTLSVA), 10 mM magnesium acetate, and 90 μM γ-^{33}P-ATP (final volume of 25 μL) for 40 minutes at room temperature. Then, the reaction was stopped with 3% phosphoric acid. 10 μL of this mixture was spotted onto a P30 filtermat and washed three times for five minutes with 75 mM phosphoric acid and once with methanol. Finally, the membrane was dried and a scintillation counter was used. An ATP concentration within 15 μM of the apparent K_m for ATP was chosen because Hayess and Benndorf showed that the mechanism of their original inhibitor peptide was not competitive with ATP binding [35].

In addition to determining the IC_{50} value for MMI-0100, inhibitory activity against 266 human kinases was tested using Millipore's IC_{50}*Profiler* Express service. For specificity analysis, a 100μM concentration of MMI-0100 was chosen for testing, as this concentration inhibited adhesion formation in the current *in vivo* study. The compound was supplied in DMSO. Every kinase activity measurement was conducted in duplicate. Individual conditions for each assay (reference inhibitors, buffer conditions, ATP concentration, substrate, etc.) and information about each kinase tested can be found on Millipore's website, at http://www.millipore.com/drugdiscovery/dd3/kpservices.

Mesothelial cell culture and treatment

A cell line of human pleural mesothelial cells (CRL-9444) was purchased from ATCC. Cells were maintained and seeded in Medium199 with Earle's BSS and 0.75 mM L-glutamine (Mediatech, Inc., Manassas, VA), 1.25 g/L sodium bicarbonate (Sigma), 3.3 nM epidermal growth factor (MBL International, Woburn, MA), 40 nM hydrocortisone (Sigma), 870 nM insulin (MBL International), 20 mM HEPES (Sigma), trace elements mixture B (Mediatech, Inc.), 10% fetal bovine serum (FBS) (Hyclone, Waltham, MA), and 1% penicillin/ streptomycin (Mediatech, Inc.). Prior to treating cells with therapeutics, cells were allowed to acclimate in serum-free medium consisting of only Medium199 with Earle's BSS, L-glutamine, sodium bicarbonate, HEPES, trace elements mixture B, and penicillin/ streptomycin (concentrations and suppliers same as above) for 24 hours prior to treatment with cytokines and/or MK2 inhibitor peptide. Cytokines with or without inhibitor peptide were also always added simultaneously in this medium formulation. The cell-penetrating MK2 inhibitor peptide YARAAARQARAKALARQLGVAA (MMI-0100, IC50 = 22 μM) was used.

IL-6 ELISA analysis

The IL-6 ELISA kit was supplied by PeproTech, Inc. (Rocky Hill, NJ). Chemicals for buffers and the ABTS liquid substrate solution were attained from Sigma. Compound reconstitution and volume additions to each well were in accordance with the manufacturer’s instructions for each lot. All experiments were performed at room temperature and all incubation steps took place on a plate shaker adjusted to 300 rpm. Nunc MaxiSorp microplates were coated with the appropriate capture antibody overnight. Blocking, sample and standard incubation, detection antibody addition, and avidin-horseradish peroxidase conjugate addition were completed in accordance with the manufacturer’s instructions. After substrate solution addition, absorbance was measured at 405 nm and 650 nm (650 nm was the wavelength correction subtracted from each 405 nm measurement) using a Spectramax M5 Microplate Reader (Molecular Devices) every 5 minutes for 50 minutes. The time point for data analysis was selected in accordance with manufacturer recommendations. Hoeschst 33342 nuclear stain (Invitrogen) was used to quantify cell number on the basis of DNA quantity. All results were run in triplicate and normalized to cell number.

In-cell Western analysis for HSPB1 phosphorylation

Mesothelial cells were seeded at a density of 200,000 cells/ml in 96-well clear bottom black well Cell Bind plates (Corning). Once confluent, cells were treated with serum free medium for 24 hours. Following a change of media, cells were either left untreated (negative control) or treated with 1 ng/ml interleukin-1β (Peprotech) and/or 1000μM MMI-0100 and/or 5μM AKT Inhibitor (EMD Chemicals). After six hours, media samples were removed for ELISA analysis and the cells were fixed with formaldehyde, permeabilized with 0.1% Triton X in TBS, blocked for 90 minutes with gentle rotation in Odyssey Blocking Buffer, and incubated with primary antibodies overnight at 4°C with gentle rocking. The specificity of all primary antibodies was confirmed via standard Western blot before use in all in-cell Westerns. The following primary antibodies were used: HSPB1 monoclonal antibody (1:833) (G3.1) (Stressgen), HSPB1 phospho S15 antibody (1:250) (Abcam), HS27 phospho S78 antibody [Y175] (1:500) (Abcam), and Phospho-HSPB1 Ser 82 (1:125) (Cell Signaling). After washing five times with 0.1% Tween-20 in TBS, samples were incubated with secondary antibodies for one hour (IRDye 680 goat antimouse (1:200; Li-Cor) and IRDye 800CW goat anti-rabbit (1:800; Li-Cor). After five washes with 0.1% Tween-20 in TBS, samples were visualized on a Li-Cor Odyssey system. The Odyssey software was used to quantify the intensity of each channel. Secondary-only controls were used to subtract off background intensity from each sample. All samples were run in quadruplicate. Statistical

significance was determined with a one-way ANOVA, with a significance level of α=0.05. A Bonferroni post-hoc test was used to determine which samples differed significantly from IL-1β only treated samples.

Western blot analysis for hNRNPA0 phosphorylation

Mesothelial cells were seeded at a density of 200,000 cells/ml in 35mm tissue culture dishes. Once confluent, the cells were treated with serum free medium for 24 hours. Following a change of medium, cells were treated with 1 ng/ml interleukin-1β (Peprotech) and/or 1000μM or 3000μM MMI-0100. After 6 and 12 hours, cells were washed twice with ice cold TBS and collected in lysis buffer (9 M Urea, 4% CHAPA, 100 μl Sigma Phosphatase Inhibitor Cocktail 1) using a cell scraper. The lysates were frozen at −80°C and vortexed in a disruptor genie for three hours at 4°C to disrupt the cell membrane. The membrane components were pelleted via centrifugation. A BCA assay was used to determine the total protein concentration of each sample. Protein (20μg) was run on 12% polyacrylamide gels at 65V, transferred onto a nitrocellulose membrane using a transblot SD semi-dry system (Biorad), blocked with 1:1 Odyssey Blocking buffer and TBS for one hour, and incubated with anti-phospho hnRNPA0 (Ser84) (1:558) (Upstate) and β-actin (1:1000; Abcam). After 4 washes, the blots were probed with secondary antibodies (IRDye 680 goat anti-mouse(1:5000; Li-Cor) and IRDye 800CW goat anti-rabbit (1:500; Li-Cor)) and visualized with the Licor Odyssey system. The Odyssey Software was used to quantify the band intensity. hNRNPA0 expression was normalized to β-actin for each lane.

In vivo model of intra-abdominal adhesion formation

We used a standard model of colon transection and anastomosis [40] for evaluating the effect of MMI-0100 on adhesion formation. This provides a reproducible model of adhesion formation while also allowing for the evaluation of anastomotic healing, which is often compromised by anti-adhesion therapies. This injury model elicits an intra-peritoneal inflammatory response similar to clinical surgery and also starts fibrinogenesis, which is critical to the early phase of adhesion formation.

Briefly, under Ketamine and Xylazine (IM) anesthesia, the abdomen was shaved, prepped with organic iodine solution, and a midline incision was performed. The descending colon was divided sharply three centimeters above the peritoneal reflection and a single layer, hand-sewn colonic anastomosis was performed using interrupted inverting 6-0 Prolene sutures. Treatment with the MK2 inhibitor peptide MMI-0100 (100 μM solution in PBS) or with PBS was carried out by spraying 5 ml over the anastomotic site, as well as the rest of the visceral contents of the abdomen. The fascia was reapproximated with continuous silk suture.

At sacrifice, using a paramedian incision to avoid disrupting adhesions underlying the incision site, the abdomen was accessed. Anastomotic healing was assessed by measuring colon bursting pressure and anastomotic collagen content while adhesions were graded by two observers blinded to the treatment, using a scoring system developed by Mazuji, et al. [41] (Table 1), with the addition of a category for number of organs involved in adhesions to capture both the tenacity of the adhesion and the number of adhesions formed. The colon distal to the anastomosis was tied off and the proximal end was divided, taking care not to disturb the peri-anastomotic adhesions and an angiocath, connected to a pressure transducer, was inserted into the lumen and secured with a silk tie. A continuous infusion of normal saline (2 ml/min) into the isolated colonic segment was carried out and bursting pressures were digitally recorded and identified as the highest pressure obtained just prior to visible leak or sudden pressure drop. After scoring adhesions, the colon anastomotic segment (5mm

proximal and distal to the suture line) was resected, dissected clean of adhesions, and stored at −20°C for analysis for hydroxyproline content as an index of newly synthesized collagen.

The scoring system (Table 1) for evaluating adhesions assessed two aspects of adhesion formation: it first scored the quality and tenacity of the adhesions formed as: 1= light, flimsy, easily dissected, 2= moderate, adherent, some force, 3= heavy, sharp dissection required, 4= severe, not dissectable without damaging structures. Second, the number of organs involved in adhesion formation was evaluated, with one point given for each of the following organs involved: epididymal fat, small bowel, omentum, colon or the abdominal wall. Thus, these scores ranged from 0 to 9, providing a broad enough scale for evaluating the effects of MMI-0100 therapy.

Hydroxyproline assay

The assay was developed using the methods of Reddy and Enwemeka [42]. All anastomotic samples were weighed and hydrolyzed in 6N HCl overnight at 110° C. The following day, the samples were gravity filtered and titrated to a neutral pH using a NaOH buffer. A 0.05M chloramine T solution was added to all the samples, followed by a 3.15M solution of perchloric acid. Finally, para-dimethylaminebenzaldehyde (20% solution) was added and the samples were placed in a warm water bath. After 20 minutes, the samples were cooled in tap water and the absorbency of the samples was tested on the spectrometer at 560 nm.

Statistical analysis

All results presented are means ± standard deviation. One-way ANOVA analyses were used to determine statistically significant increases or decreases in parameters of interest. Significant differences were analyzed with Tukey HSD post hoc comparisons, unless otherwise described above. In all cases, a significance level of $\alpha = 0.05$ was used.

Results

MMI-0100 IC_{50} and specificity

The IC50 of MMI-0100 was determined to be 22 μM. In addition to determining the IC50 of the compound, we examined its specificity of kinase inhibition. To do this, we tested all 266 human kinases available for testing in the Millipore kinase profiling service cited above. At 100 μM, the peptide inhibited greater than 65% of activity of only 17 wild-type kinases (data not shown). Eight of seventeen of the kinases that inhibited greater than 65% are, as is MK2, members of the calcium/calmodulin-dependent protein kinase family; in addition, four are members of the tyrosine kinase family and three are members of the cAMP-dependent, cGMP-dependent and protein kinase C (AGC) family.

IL-1β and TNF-α upregulated IL-6 expression in a time- and dose-dependent manner in mesothelial cells

To determine doses and time intervals that significantly upregulated IL-6 expression, mesothelial cells were treated with 0.1, 1, or 10 ng/mL of IL-1β and TNF-α for 2, 6, 12, and 24 hours (Fig. 1a & 1b). Without IL-1β or TNF-α stimulation, mesothelial cells made negligible amounts of IL-6; however, both IL-1β and TNF-α increased IL-6 expression in a time- and dose-dependent manner. All three concentrations of IL-1β significantly increased IL-6 expression after six hours ($p<0.05$), but by 24 hours, the two higher concentrations of IL-1β induced similar levels of IL-6 expression. Since investigators have previously established 1 ng/mL IL-1β as the most physiologically-relevant concentration for mesothelial cells [43], subsequent experiments also employed 1 ng/mL IL-1β. Excluding the 24-hour time point for the highest dose of TNF-α used, TNF-α was a less potent inducer of IL-6 expression than IL-1β. The 0.1 ng/mL dose of TNF-α rarely produced significant

increases in IL-6. Even the 1 ng/mL TNF-α dose did not always significantly upregulate IL-6 expression above the untreated control. Thus, in subsequent experiments, 10 ng/mL TNF-α was selected as the stimulant. Ten ng/mL TNF-α is also regarded as most physiologically relevant concentration for mesothelial cells [43].

High dose of MMI-0100 attenuated IL-1β-induced IL-6 expression at multiple time points

To show that YARAAARQARAKALARQLGVAA (MMI-0100) inhibited IL-1β-induced IL-6 expression in mesothelial cells, mesothelial cells were treated with two concentrations of MMI-0100 (Figure 2). At the highest concentration tested, MMI-0100 significantly reduced IL-1β-induced IL-6 expression ($p<0.05$) at all three time points examined. However, at the latter two time points, overall IL-6 expression was still significantly higher than the untreated baseline ($p<0.05$). Lower concentrations of MMI-0100 (1000 μM) appeared to reduce IL-1β-induced IL-6 expression in a dose dependent manner, but only the highest concentration was able to significantly reduce IL-6 expression.

MMI-0100 inhibits IL-6 expression induced by TNF-α at multiple time points

To show that MMI-0100 opposed TNF-α-induced IL-6 expression in mesothelial cells, mesothelial cells were treated with 3,000 μM or 1,000 μM of MMI-0100 and 10 ng/ml TNF-α (Figure 3). In mesothelial cells treated with 10 ng/mL TNF-α, the peptide was effective in reducing TNF-α induced IL-6 expression ($p<0.05$). At every time point, the higher MMI-0100 dose reduced IL-6 expression levels to that of the untreated baseline.

MMI-0100 inhibits IL-1β-induced phosphorylation of hnRNPA0 in mesothelial cells

Treatment of mesothelial cells with 1 ng/ml IL-1β induced a 2-fold upregulation of phosphorylated transcription factor hnRNPA0, a substrate of MK2, as compared to controls at 6 hours.Simultaneous treatment with MMI-0100 reduced the level of phosphorylation, with 3000 μM MMI-0100 reducing the level of hnRNPA0 phosphorylation to that of the untreated controls (Figure 4). At 12 hours, treatment with IL-1β no longer upregulates the phosphorylation of hnRNPA0.

MMI-0100 inhibits phosphorylation of HSPB1 S15 and AKT inhibitor attenuates phosphorylation of HSPB1 Ser82 in mesothelial cells

Neither MMI-0100 nor AKT inhibitor decrease the phosphorylation of HSPB1 on S78 (data not shown). MMI-0100 did attenuate S15 phosphorylation following stimulation with IL1-β ($p<0.05$), while AKT had no effect on S15 phosphorylation (Figure 5a). However, consistent with other published studies, the AKT inhibitor reduced the level of HSPB1 phosphorylation on S82 ($p<0.05$). MMI-0100 did not affect HSPB1 S82 phosphorylation (Figure 5b).

In vivo inhibition of adhesion formation

A total of three animals were lost from the study. Two animals were lost from the control group: one from a transverse colonic volvulus 5 days after surgery and one from an anastomotic leak 7 days after surgery. One animal was lost from the treatment group on day six, although autopsy showed no obvious reason for death.

In all cases, as shown in Table 2, a single treatment with MMI-0100 at the time of surgery did not significantly affect rat weight gain, anastomosis bursting pressure or intestinal hydroxyproline (OHP) content at either time point, demonstrating a lack of negative impact on normal healing. However, the peptide-treated rats had significantly lower adhesion incidence and density scores at 10-days ($P<0.005$).

Discussion

These studies describe the activity of a cell-penetrating peptide inhibitor of MK2, MMI-0100. Cell studies validated that the peptide inhibits many of the functions attributed to MK2. *In vitro* studies demonstrated that MMI-0100 has an IC50 value of 22μM, which was shown in our rat model to be therapeutically relevant for inhibiting adhesion formation as a result of bowel anastomosis surgery. While the peptide is not 100% specific for MK2, it does appear to be relatively specific to a subset of CaMKs and TKs. Both the *in vitro* data demonstrating suppress inflammatory cytokine expression and the known correlation between inflammation and adhesions suggest that MK2 inhibitor activity of the peptide is a major factor in the therapeutics ability to downregulate adhesion formation *in vivo*. In addition, there were no obvious *in vivo* side effects including labored breathing, vomiting, loss of appetite or weight loss as a result of treating animals with MMI-0100 for the purpose of inhibiting surgically induced adhesions.

To verify that MMI-0100 inhibited functions attributed to MK2 in a medically relevant cell line, we investigated the ability of a human mesothelial cell line to express IL-6 in response to inflammatory cytokine expression. As discussed earlier, IL-6 expression is important in abdominal adhesion formation. Consistent with published studies, both IL-1β and TNF-α increased mesothelial cell IL-6 expression [44–46]. These cited studies and our results also established that, without stimulation, mesothelial cells made very small amounts of IL-6. Consistent with other studies using human peritoneal mesothelial cells [44,45], IL-1β was a more potent inducer of IL-6 expression than TNF-α.

Next, we confirmed that MMI-0100 diminished IL-1β and TNF-α induced IL-6 expression by mesothelial cells. At the highest concentration tested, MMI-0100 significantly reduced IL-1β-induced IL-6 expression ($p<0.05$). However, the MK2 inhibitor peptide was much more effective in reducing TNF-α-induced IL-6 expression at all three time points examined as compared to reducing IL-1β-induced expression. The highest concentration of peptide used in these studies was well below the toxic dose for mesothelial cells [37]. This concentration was effective in bringing TNF-α-induced IL-6 expression to baseline levels or below but not effective in bringing IL-1β-induced IL-6 expression to baseline levels. The peptide acted at all time points to reduce IL-6 expression in response to both TNF-α and IL-1β. While the MK2 inhibitor used in this study is not completely specific for MK2 [37,47], the ability of the compound to inhibit IL-1β- and TNF-α-induced IL-6 expression provides strong evidence that the compound did inhibit the actions of MK2 based on the link between MK2 and IL-6 expression.

As further evidence that the peptide inhibited MK2 in mesothelial cell culture, we analyzed the phosphorylation of hnRNPA0 after stimulation with IL-1β and treatment with or without MK2 inhibitor. Consistent with other studies, we found that hnRNPA0 was phosphorylated at serine 82 upon inflammatory cytokine stimulation and that inhibition of MK2 activity with MMI-0100 decreased the phosphorylation of hnRNPA0. Coupled with the decrease in IL6 expression and our *in vitro* kinase inhibition data, there is strong evidence that MMI-0100 is inhibiting MK2.

In addition to its role in inflammatory cytokine expression, MK2 has been associated with phosphorylation of HSPB1 (HSP25 in mice), a heat shock protein associated with stress resistance and actin cytoskeletal organization, at three serine residues (S82, S78 and S15) [48–56]. Thus, we examined the ability of the peptide to inhibit phosphorylation of HSPB1. MK2 phosphorylates HSPB1 directly in a test tube [36,57], and has been shown to phosphorylate HSPB1 in cells, as well [52–56]. Our data suggest that the concentration of MK2 inhibitor peptide that is effective at suppressing MK2 activity *in vitro* and that

attenuates hnRNPA0 phosphorylation and IL-6 expression, inhibits HSPB1 phosphorylation at S15, but not at S78 nor at S82 in mesothelial cells. This contradicts many published studies using knockout mice and cells derived from these animals, which show that MK2 directly phosphorylates HSPB1 at all 3 serines [58,59]. Interestingly, recent work by Revesz *et al.* has shown that small molecule inhibitors of MK2, with known off-target kinase inhibition activity, show order of magnitude differences in their IC50 values against cytokine expression and HSPB1 phosphorylation [60]. Our data suggest that either greater inhibitor concentrations are needed for inhibition of HSPB1 phosphorylation at S78 and S82 than are needed to inhibit cytokine expression and HSPB1 S15 and hnRNPA0 phosphorylation, or that some other kinase is responsible for HSPB1 phosphorylation at sites S78 and S82 in cells. Recent evidence suggests that HSPB1 can be phosphorylated by multiple other kinases, including p38 regulated/activated protein kinase (PRAK), which phosphorylates HSPB1 at the same sites as MK2 [61,62]. Like MK2, the serine/threonine kinase Akt phosphorylates S82 in response to p38 pathway activators [63] and protein kinase D (PKD) also phosphorylates S82 [64]. In response to oxidative stress, PKCδ phosphorylates HSPB1 at serines 82 and 15 [65,66].

To test whether another kinase may be responsible for phosphorylation HSPB1 in cells, we examined the ability of an inhibitor of AKT to suppress HSPB1 phosphorylation at HSPB1 Ser82. We found that the AKT inhibitor downregulated S82 phosphorylation to baseline levels, as does dual AKT and MK2 inhibition, while again, MK2 inhibition alone was unable to suppress S82 phosphorylation. These data suggest that, while MK2 is able to inhibit phosphorylation at all three serine residues in a test tube, it may not be responsible for phosphorylating S78 and S82 *in vivo*.

Studies by Rane *et al.* [67] demonstrated that AKT inhibits phosphorylation of HSPB1 at serine 82. Since activated MK2 forms a complex with p38 MAPK, AKT, and HSPB1 [68], it is possible that MK2 activation is required for formation of this complex. Once the complex is formed, AKT is able to phosphorylate HSPB1 at serine 82. If this is the case, it would explain why MK2 knockout studies show suppressed HSPB1 phosphorylation at Ser82. Additional studies are needed to demonstrate whether this hypothesis is true. Complicating the issue is the fact that no completely specific MK2 inhibitor is available and siRNA and knockout studies complete eliminate MK2 expression, which inhibits both protein-protein interactions and kinase activity.

The ability of MK2 peptide inhibitor to significantly decrease adhesions in an intestinal anastomosis model without affecting the mechanical properties of the intestine or normal healing is significant. The market leader in adhesion prevention products, Seprafilm®, as well as Adept, the only other FDA approved product to treat abdominal adhesions, are specifically contraindicated for intestinal anastomosis [2,69]. According to the product label, Seprafilm® “should not be wrapped directly around a fresh anastomotic suture or staple line”[70]. In this application, Seprafilm® is associated with anastomotic leakage [70,71]. In colorectal resections or adhesiolysis, Seprafilm® also caused significantly more fistulas and peritonitis in patients [70]. In these initial studies, MMI-0100 did not cause any of these complications in this rat anastomosis model and may represent a novel way to decrease the severity and incidence of adhesions at the time of anastomotic surgery without inciting additional complications for the patient.

In conclusion, we developed a cell-penetrating peptide inhibitor of MK2 (MMI-0100). This peptide inhibited IL-1β- and TNF-α-induced IL-6 expression in human pleural mesothelial cells. The *in vivo* bowel anastomosis model demonstrated that the MMI-0100 peptide has the potential to reduce both the incidence and severity of abdominal adhesions resulting

from bowel anastomosis surgery. Further investigation of the peptide for inhibition of abdominsal adhesions is warranted.

Acknowledgments

This research was supported in part by the NIH (National Institutes of Health; Bethesda, MD, U.S.A.) (grant number K25HL074968) and the Purdue Research Foundation Trask Innovation Fund. B.W. was supported in part by an NIH Medical Scientist Training Program grant (grant number GM077229) and by the Purdue Research Foundation. Moerae Matrix supported the animal studies and kinase profiling. J.B. is supported by an NSF Graduate Research Fellowship.

REFERENCES

1. Ellis H. The clinical significance of adhesions: focus on intestinal obstruction. Eur J Surg Suppl. 1997; (577):5–9. [PubMed: 9076446]
2. Frost, Sullivan. U.S. Markets for Hemostats - Tissue Sealants-Tissue Adhesives and Adhesion Prevention Products. 2004 December.
3. Ray NF, Denton WG, Thamer M, Henderson SC, Perry S. Abdominal adhesiolysis: inpatient care and expenditures in the United States in 1994. J Am Coll Surg. 1998; 186(1):1–9. [PubMed: 9449594]
4. DeFrances, CJ.; Podgornik, MN. Center for Disease Control and Prevention. Services USDoHaH: Center for Disease Control and Prevention; 2006. 2004 National Hospital Discharge Survey. In. Edited by
5. Kishimoto T. The biology of interleukin-6. Blood. 1989; 74(1):1–10. [PubMed: 2473791]
6. Cheong YC, Shelton JB, Laird SM, Richmond M, Kudesia G, Li TC, Ledger WL. IL-1, IL-6 and TNF-alpha concentrations in the peritoneal fluid of women with pelvic adhesions. Hum Reprod. 2002; 17(1):69–75. [PubMed: 11756364]
7. Chegini N. Peritoneal molecular environment, adhesion formation and clinical implication. Front Biosci. 2002; 7:e91–e115. [PubMed: 11897550]
8. Saba AA, Kaidi AA, Godziachvili V, Dombi GW, Dawe EJ, Libcke JH, Silva YJ. Effects of interleukin-6 and its neutralizing antibodies on peritoneal adhesion formation and wound healing. Am Surg. 1996; 62(7):569–572. [PubMed: 8651553]
9. Cheong YC, Laird SM, Shelton JB, Ledger WL, Li TC, Cooke ID. The correlation of adhesions and peritoneal fluid cytokine concentrations: a pilot study. Hum Reprod. 2002; 17(4):1039–1045. [PubMed: 11925402]
10. Buyalos RP, Funari VA, Azziz R, Watson JM, Martinez-Maza O. Elevated interleukin-6 levels in peritoneal fluid of patients with pelvic pathology. Fertil Steril. 1992; 58(2):302–306. [PubMed: 1633894]
11. Houssiau FA, Devogelaer JP, Van Damme J, de Deuxchaisnes CN, Van Snick J. Interleukin-6 in synovial fluid and serum of patients with rheumatoid arthritis and other inflammatory arthritides. Arthritis Rheum. 1988; 31(6):784–788. [PubMed: 3260102]
12. Hegen M, Gaestel M, Nickerson-Nutter CL, Lin LL, Telliez JB. MAPKAP kinase 2-deficient mice are resistant to collagen-induced arthritis. J Immunol. 2006; 177(3):1913–1917. [PubMed: 16849504]
13. Houssiau FA, Bukasa K, Sindic CJ, Van Damme J, Van Snick J. Elevated levels of the 26K human hybridoma growth factor (interleukin 6) in cerebrospinal fluid of patients with acute infection of the central nervous system. Clin Exp Immunol. 1988; 71(2):320–323. [PubMed: 3349651]
14. Kawano M, Hirano T, Matsuda T, Taga T, Horii Y, Iwato K, Asaoku H, Tang B, Tanabe O, Tanaka H, et al. Autocrine generation and requirement of BSF-2/IL-6 for human multiple myelomas. Nature. 1988; 332(6159):83–85. [PubMed: 3258060]
15. Miki S, Iwano M, Miki Y, Yamamoto M, Tang B, Yokokawa K, Sonoda T, Hirano T, Kishimoto T. Interleukin-6 (IL-6) functions as an in vitro autocrine growth factor in renal cell carcinomas. FEBS Lett. 1989; 250(2):607–610. [PubMed: 2787758]

16. Yokoyama A, Kohno N, Fujino S, Hamada H, Inoue Y, Fujioka S, Ishida S, Hiwada K. Circulating interleukin-6 levels in patients with bronchial asthma. Am J Respir Crit Care Med. 1995; 151(5): 1354–1358. [PubMed: 7735584]

17. Tamm I, Cardinale I, Krueger J, Murphy JS, May LT, Sehgal PB. Interleukin 6 decreases cell-cell association and increases motility of ductal breast carcinoma cells. J Exp Med. 1989; 170(5): 1649–1669. [PubMed: 2553849]

18. Hirano T, Taga T, Yasukawa K, Nakajima K, Nakano N, Takatsuki F, Shimizu M, Murashima A, Tsunasawa S, Sakiyama F, et al. Human B-cell differentiation factor defined by an anti-peptide antibody and its possible role in autoantibody production. Proc Natl Acad Sci U S A. 1987; 84(1): 228–231. [PubMed: 3491991]

19. Erroi A, Sironi M, Chiaffarino F, Chen ZG, Mengozzi M, Mantovani A. IL-1 and IL-6 release by tumor-associated macrophages from human ovarian carcinoma. Int J Cancer. 1989; 44(5):795–801. [PubMed: 2583859]

20. Gastl G, Plante M, Finstad CL, Wong GY, Federici MG, Bander NH, Rubin SC. High IL-6 levels in ascitic fluid correlate with reactive thrombocytosis in patients with epithelial ovarian cancer. Br J Haematol. 1993; 83(3):433–441. [PubMed: 8485049]

21. Kutteh WH, Kutteh CC. Quantitation of tumor necrosis factor-alpha, interleukin-1 beta, and interleukin-6 in the effusions of ovarian epithelial neoplasms. Am J Obstet Gynecol. 1992; 167(6): 1864–1869. [PubMed: 1471711]

22. Scambia G, Testa U, Panici PB, Martucci R, Foti E, Petrini M, Amoroso M, Masciullo V, Peschle C, Mancuso S. Interleukin-6 serum levels in patients with gynecological tumors. Int J Cancer. 1994; 57(3):318–323. [PubMed: 8168990]

23. Culbert AA, Skaper SD, Howlett DR, Evans NA, Facci L, Soden PE, Seymour ZM, Guillot F, Gaestel M, Richardson JC. MAPK-activated protein kinase 2 deficiency in microglia inhibits pro-inflammatory mediator release and resultant neurotoxicity. Relevance to neuroinflammation in a transgenic mouse model of Alzheimer disease. J Biol Chem. 2006; 281(33):23658–23667. [PubMed: 16774924]

24. Gorska MM, Liang Q, Stafford SJ, Goplen N, Dharajiya N, Guo L, Sur S, Gaestel M, Alam R. MK2 controls the level of negative feedback in the NF-kappaB pathway and is essential for vascular permeability and airway inflammation. J Exp Med. 2007; 204(7):1637–1652. [PubMed: 17576778]

25. Jagavelu K, Tietge UJ, Gaestel M, Drexler H, Schieffer B, Bavendiek U. Systemic deficiency of the MAP kinase-activated protein kinase 2 reduces atherosclerosis in hypercholesterolemic mice. Circ Res. 2007; 101(11):1104–1112. [PubMed: 17885219]

26. Kontoyiannis D, Boulougouris G, Manoloukos M, Armaka M, Apostolaki M, Pizarro T, Kotlyarov A, Forster I, Flavell R, Gaestel M, et al. Genetic dissection of the cellular pathways and signaling mechanisms in modeled tumor necrosis factor-induced Crohn's-like inflammatory bowel disease. J Exp Med. 2002; 196(12):1563–1574. [PubMed: 12486099]

27. Kotlyarov A, Neininger A, Schubert C, Eckert R, Birchmeier C, Volk HD, Gaestel M. MAPKAP kinase 2 is essential for LPS-induced TNF-alpha biosynthesis. Nat Cell Biol. 1999; 1(2):94–97. [PubMed: 10559880]

28. Reinhardt HC, Aslanian AS, Lees JA, Yaffe MB. p53-deficient cells rely on ATM- and ATR-mediated checkpoint signaling through the p38MAPK/MK2 pathway for survival after DNA damage. Cancer Cell. 2007; 11(2):175–189. [PubMed: 17292828]

29. Thomas T, Hitti E, Kotlyarov A, Potschka H, Gaestel M. MAP-kinase-activated protein kinase 2 expression and activity is induced after neuronal depolarization. Eur J Neurosci. 2008; 28(4):642–654. [PubMed: 18702688]

30. Tietz AB, Malo A, Diebold J, Kotlyarov A, Herbst A, Kolligs FT, Brandt-Nedelev B, Halangk W, Gaestel M, Goke B, et al. Gene deletion of MK2 inhibits TNF-alpha and IL-6 and protects against cerulein-induced pancreatitis. Am J Physiol Gastrointest Liver Physiol. 2006; 290(6):G1298–G1306. [PubMed: 16423921]

31. Neininger A, Kontoyiannis D, Kotlyarov A, Winzen R, Eckert R, Volk HD, Holtmann H, Kollias G, Gaestel M. MK2 targets AU-rich elements and regulates biosynthesis of tumor necrosis factor and interleukin-6 independently at different post-transcriptional levels. J Biol Chem. 2002; 277(5): 3065–3068. [PubMed: 11741878]

32. Thomas T, Timmer M, Cesnulevicius K, Hitti E, Kotlyarov A, Gaestel M. MAPKAP kinase 2-deficiency prevents neurons from cell death by reducing neuroinflammation--relevance in a mouse model of Parkinson's disease. J Neurochem. 2008; 105(5):2039–2052. [PubMed: 18298661]
33. Johansen C, Funding AT, Otkjaer K, Kragballe K, Jensen UB, Madsen M, Binderup L, Skak-Nielsen T, Fjording MS, Iversen L. Protein expression of TNF-alpha in psoriatic skin is regulated at a posttranscriptional level by MAPK-activated protein kinase 2. J Immunol. 2006; 176(3):1431–1438. [PubMed: 16424170]
34. Rousseau S, Morrice N, Peggie M, Campbell DG, Gaestel M, Cohen P. Inhibition of SAPK2a/p38 prevents hnRNP A0 phosphorylation by MAPKAP-K2 and its interaction with cytokine mRNAs. The EMBO journal. 2002; 21(23):6505–6514. [PubMed: 12456657]
35. Hayess K, Benndorf R. Effect of protein kinase inhibitors on activity of mammalian small heat-shock protein (HSP25) kinase. Biochem Pharmacol. 1997; 53(9):1239–1247. [PubMed: 9214684]
36. Lopes LB, Flynn C, Komalavilas P, Panitch A, Brophy CM, Seal BL. Inhibition of HSP27 phosphorylation by a cell-permeant MAPKAP Kinase 2 inhibitor. Biochem Biophys Res Commun. 2009; 382(3):535–539. [PubMed: 19289101]
37. Ward BC, Seal BL, Brophy CM, Panitch A. Design of a bioactive cell-penetrating, peptide: when a transduction domain does more than transduce. Journal of Peptide Science. 2009
38. Ho A, Schwarze SR, Mermelstein SJ, Waksman G, Dowdy SF. Synthetic protein transduction domains: enhanced transduction potential in vitro and in vivo. Cancer Res. 2001; 61(2):474–477. [PubMed: 11212234]
39. Bodanszky, M. Peptide chemistry: a practical textbook. Berlin ; New York: Springer-Verlag; 1988.
40. Snoj M. Effect of phosphatidylcholine on postoperative adhesions after small bowel anastomosis in the rat. British journal of surgery. 1992; 79(5):427. [PubMed: 1596725]
41. Mazuji M, Kalambaheti K, Pawar B. Prevention of adhesions with polyvinylpyrrolidone - preliminary report. Archives of surgery. 1964; 89(6):1011–1015. [PubMed: 14208444]
42. Reddy GK, Enwemeka CS. A simplified method for the analysis of hydroxyproline in biological tissues. Clin Biochem. 1996; 29(3):225–229. [PubMed: 8740508]
43. Visser CE, Steenbergen JJ, Betjes MG, Meijer S, Arisz L, Hoefsmit EC, Krediet RT, Beelen RH. Interleukin-8 production by human mesothelial cells after direct stimulation with staphylococci. Infect Immun. 1995; 63(10):4206–4209. [PubMed: 7558346]
44. Topley N, Jorres A, Luttmann W, Petersen MM, Lang MJ, Thierauch KH, Muller C, Coles GA, Davies M, Williams JD. Human peritoneal mesothelial cells synthesize interleukin-6: induction by IL-1 beta and TNF alpha. Kidney Int. 1993; 43(1):226–233. [PubMed: 8433563]
45. Offner FA, Obrist P, Stadlmann S, Feichtinger H, Klingler P, Herold M, Zwierzina H, Hittmair A, Mikuz G, Abendstein B, et al. IL-6 secretion by human peritoneal mesothelial and ovarian cancer cells. Cytokine. 1995; 7(6):542–547. [PubMed: 8580370]
46. Lanfrancone L, Boraschi D, Ghiara P, Falini B, Grignani F, Peri G, Mantovani A, Pelicci PG. Human peritoneal mesothelial cells produce many cytokines (granulocyte colony-stimulating factor [CSF], granulocyte-monocyte-CSF, macrophage-CSF, interleukin-1 [IL-1], and IL-6) and are activated and stimulated to grow by IL-1. Blood. 1992; 80(11):2835–2842. [PubMed: 1280480]
47. Davies SP, Reddy H, Caivano M, Cohen P. Specificity and mechanism of action of some commonly used protein kinase inhibitors. Biochem J. 2000; 351(Pt 1):95–105. [PubMed: 10998351]
48. Kobayashi M, Nishita M, Mishima T, Ohashi K, Mizuno K. MAPKAPK-2-mediated LIM-kinase activation is critical for VEGF-induced actin remodeling and cell migration. Embo J. 2006; 25(4): 713–726. [PubMed: 16456544]
49. Sousa AM, Liu T, Guevara O, Stevens J, Fanburg BL, Gaestel M, Toksoz D, Kayyali US. Smooth muscle alpha-actin expression and myofibroblast differentiation by TGFbeta are dependent upon MK2. J Cell Biochem. 2006
50. Vardouli L, Moustakas A, Stournaras C. LIM-kinase 2 and cofilin phosphorylation mediate actin cytoskeleton reorganization induced by transforming growth factor-beta. J Biol Chem. 2005; 280(12):11448–11457. [PubMed: 15647284]

51. Schneider GB, Hamano H, Cooper LF. In vivo evaluation of hsp27 as an inhibitor of actin polymerization: hsp27 limits actin stress fiber and focal adhesion formation after heat shock. J Cell Physiol. 1998; 177(4):575–584. [PubMed: 10092210]
52. Stokoe D, Engel K, Campbell DG, Cohen P, Gaestel M. Identification of MAPKAP kinase 2 as a major enzyme responsible for the phosphorylation of the small mammalian heat shock proteins. FEBS Lett. 1992; 313(3):307–313. [PubMed: 1332886]
53. Landry J, Lambert H, Zhou M, Lavoie JN, Hickey E, Weber LA, Anderson CW. Human HSP27 is phosphorylated at serines 78 and 82 by heat shock and mitogen-activated kinases that recognize the same amino acid motif as S6 kinase II. J Biol Chem. 1992; 267(2):794–803. [PubMed: 1730670]
54. Clifton AD, Young PR, Cohen P. A comparison of the substrate specificity of MAPKAP kinase-2 and MAPKAP kinase-3 and their activation by cytokines and cellular stress. FEBS Lett. 1996; 392(3):209–214. [PubMed: 8774846]
55. Engel K, Ahlers A, Brach MA, Herrmann F, Gaestel M. MAPKAP kinase 2 is activated by heat shock and TNF-alpha: in vivo phosphorylation of small heat shock protein results from stimulation of the MAP kinase cascade. J Cell Biochem. 1995; 57(2):321–330. [PubMed: 7759569]
56. Schafer C, Ross SE, Bragado MJ, Groblewski GE, Ernst SA, Williams JA. A role for the p38 mitogen-activated protein kinase/Hsp 27 pathway in cholecystokinin-induced changes in the actin cytoskeleton in rat pancreatic acini. J Biol Chem. 1998; 273(37):24173–24180. [PubMed: 9727040]
57. Hayess K, Benndorf R. Effect of protein kinase inhibitors on activity of mammalian small heat shock protein (HSP25) kinase. Biochemical Pharmacology. 1997; 53(9):1239–1247. [PubMed: 9214684]
58. Ronkina N, Kotlyarov A, Dittrich-Breiholz O, Kracht M, Hitti E, Milarski K, Askew R, Marusic S, Lin LL, Gaestel M, et al. The mitogen-activated protein kinase (MAPK)-activated protein kinases MK2 and MK3 cooperate in stimulation of tumor necrosis factor biosynthesis and stabilization of p38 MAPK. Mol Cell Biol. 2007; 27(1):170–181. [PubMed: 17030606]
59. Culbert AA, Skaper SD, Howlett DR, Evans NA, Facci L, Soden PE, Seymour ZM, Guillot F, Gaestel M, Richardson JC. MAPK-activated Protein Kinase 2 Deficiency in Microglia Inhibits Pro-inflammatory Mediator Release and Resultant Neurotoxicity: Relevance to Neuroinflammation in a Transgenic Mouse Model of Alzheimer Disease. J Biol Chem. 2006; 281(33):23658–23667. [PubMed: 16774924]
60. Revesz L, Schlapbach A, Aichholz R, Feifel R, Hawtin S, Heng R, Hiestand P, Jahnke W, Koch G, Kroemer M, et al. In vivo and in vitro SAR of tetracyclic MAPKAP-K2 (MK2) inhibitors. Part I. Bioorg Med Chem Lett. 20(15):4715–4718. [PubMed: 20594847]
61. New L, Jiang Y, Zhao M, Liu K, Zhu W, Flood LJ, Kato Y, Parry GC, Han J. PRAK, a novel protein kinase regulated by the p38 MAP kinase. Embo J. 1998; 17(12):3372–3384. [PubMed: 9628874]
62. Gaestel M. MAPKAP kinases - MKs - two's company, three's a crowd. Nat Rev Mol Cell Biol. 2006; 7(2):120–130. [PubMed: 16421520]
63. Rane MJ, Pan Y, Singh S, Powell DW, Wu R, Cummins T, Chen Q, McLeish KR, Klein JB. Heat shock protein 27 controls apoptosis by regulating Akt activation. J Biol Chem. 2003; 278(30): 27828–27835. [PubMed: 12740362]
64. Doppler H, Storz P, Li J, Comb MJ, Toker A. A phosphorylation state-specific antibody recognizes Hsp27, a novel substrate of protein kinase D. J Biol Chem. 2005; 280(15):15013–15019. [PubMed: 15728188]
65. Lee YJ, Lee DH, Cho CK, Bae S, Jhon GJ, Lee SJ, Soh JW, Lee YS. HSP25 inhibits protein kinase C delta-mediated cell death through direct interaction. J Biol Chem. 2005; 280(18):18108–18119. [PubMed: 15731106]
66. Maizels ET, Peters CA, Kline M, Cutler RE Jr, Shanmugam M, Hunzicker-Dunn M. Heat-shock protein-25/27 phosphorylation by the delta isoform of protein kinase C. Biochem J. 1998; 332(Pt 3):703–712. [PubMed: 9620873]
67. Rane MJ, Coxon PY, Powell DW, Webster R, Klein JB, Pierce W, Ping P, McLeish KR. p38 Kinase-dependent MAPKAPK-2 activation functions as 3-phosphoinositide-dependent kinase-2

for Akt in human neutrophils. The Journal of biological chemistry. 2001; 276(5):3517–3523. [PubMed: 11042204]

68. Zheng C, Lin Z, Zhao ZJ, Yang Y, Niu H, Shen X. MAPK-activated protein kinase-2 (MK2)-mediated formation and phosphorylation-regulated dissociation of the signal complex consisting of p38, MK2, Akt, and Hsp27. The Journal of biological chemistry. 2006; 281(48):37215–37226. [PubMed: 17015449]
69. http://www.fda.gov/MedicalDevices/ProductsandMedicalProcedures/DeviceApprovalsandClearances/Recently-ApprovedDevices/ucm077891.htm
70. GenzymeBiosurgery. Cambridge, MA: GenzymeCorportation; 2004. Seprafilm Adhesion Barrier: Chemically Modified Sodium Hyaluronate/Carboxymethylcellulose Absorbable Adhesion Barrier. In. Edited by
71. Beck DE, Cohen Z, Fleshman JW, Kaufman HS, van Goor H, Wolff BG. A prospective, randomized, multicenter, controlled study of the safety of Seprafilm adhesion barrier in abdominopelvic surgery of the intestine. Dis Colon Rectum. 2003; 46(10):1310–1319. [PubMed: 14530667]

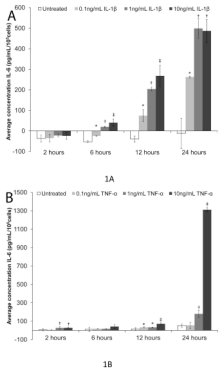

Figure 1. IL-6 expression versus time and IL-1β or TNF-α dose in mesothelial cells

(A) IL-1β and (B) TNF-α increased IL-6 expression in a time and dose-dependent manner. Single factor ANOVAs were conducted within each time interval with $p<0.05$. * = significantly higher than only untreated. † = significantly higher than both untreated and 0.1 ng/mL IL-1β or TNF-α treated. ‡ = significantly higher than all other treatments. Error bars represent standard deviation between three samples.

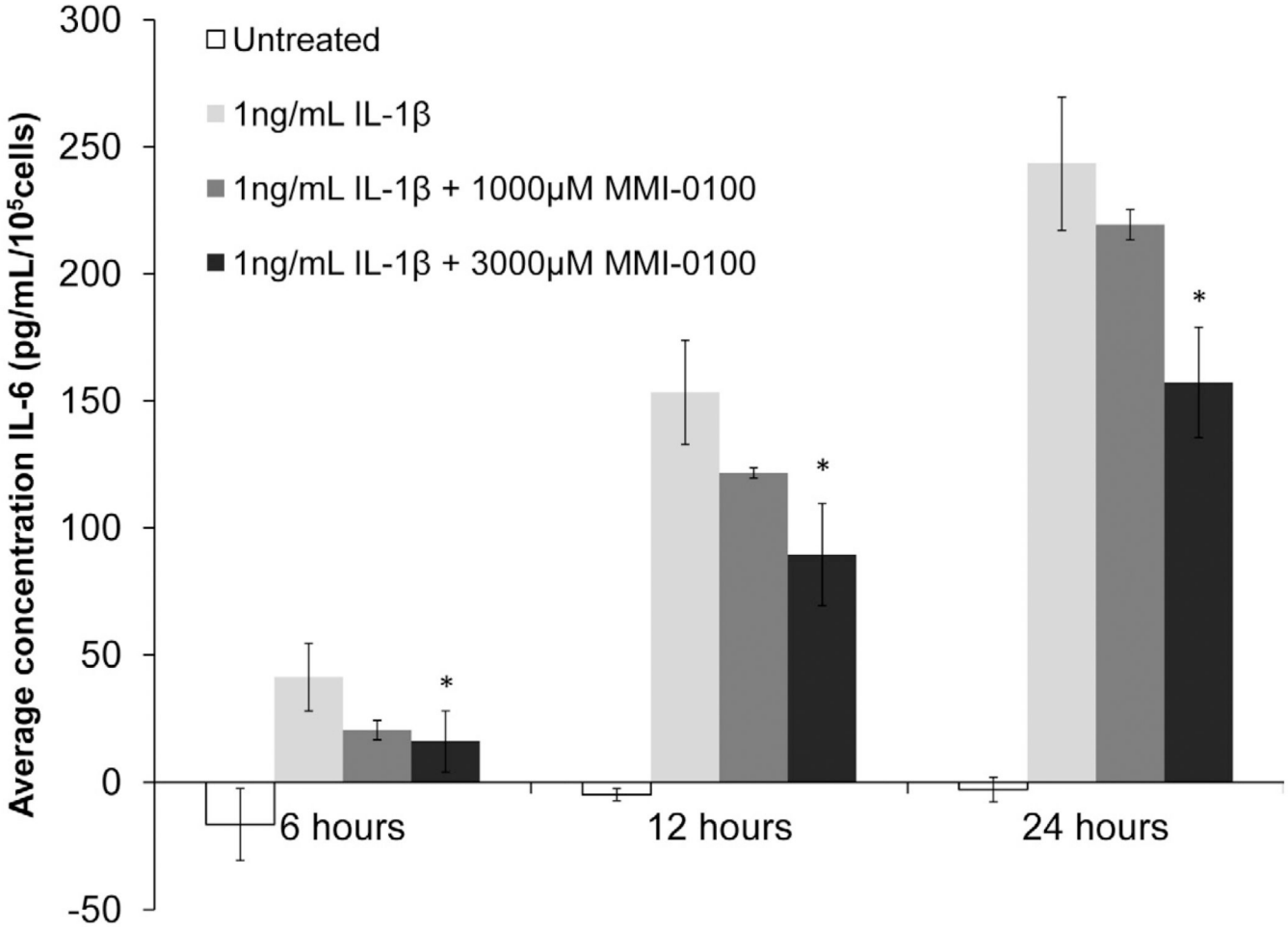

Figure 2. IL-6 expression versus treatment with 1ng/ml IL-1β or 1ng/ml IL-1β + MMI-0100 in mesothelial cells

MMI-0100, at a concentration of 3,000 μM, significantly reduced IL-1β induced IL-6 expression at all time points.. Single factor ANOVAs were conducted within each time interval with $p<0.05$. * = significantly lower than 1 ng/mL IL-1β treated samples. Error bars represent standard deviation between three samples.

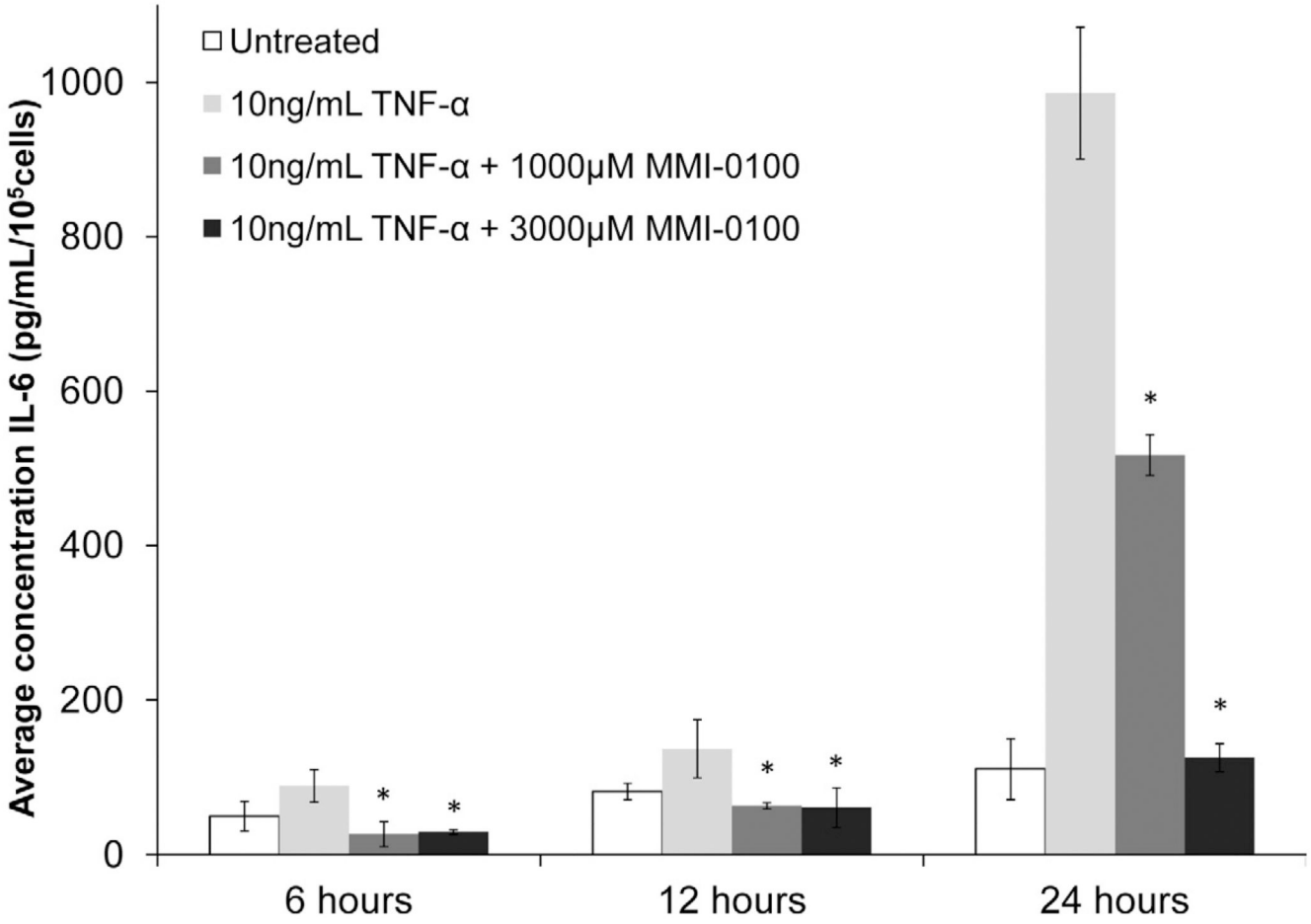

Figure 3. IL-6 expression versus treatment with 10 ng/mL TNF-α or 10 ng/mL TNF-α + MMI-0100 in mesothelial cells

Both 3,000 and 1,000 μM MMI-0100 significantly reduced TNF-α induced IL-6 expression in mesothelial cells at all three time points.. Single factor ANOVAs were conducted within each time interval with $p<0.05$. * = significantly lower than 10 ng/mL TNF-α treated samples. Error bars represent standard deviation between three samples.

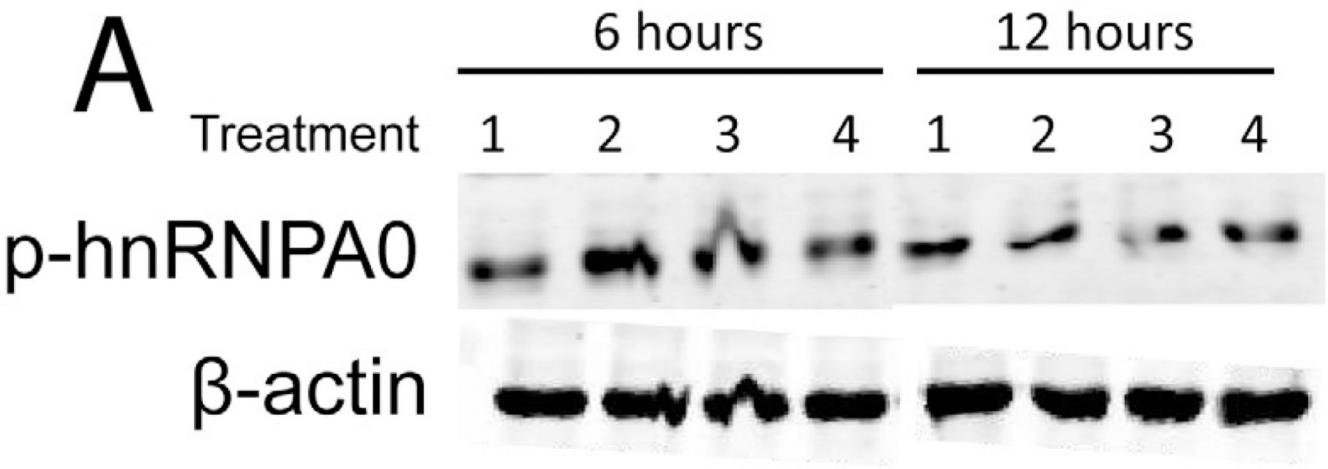

4a

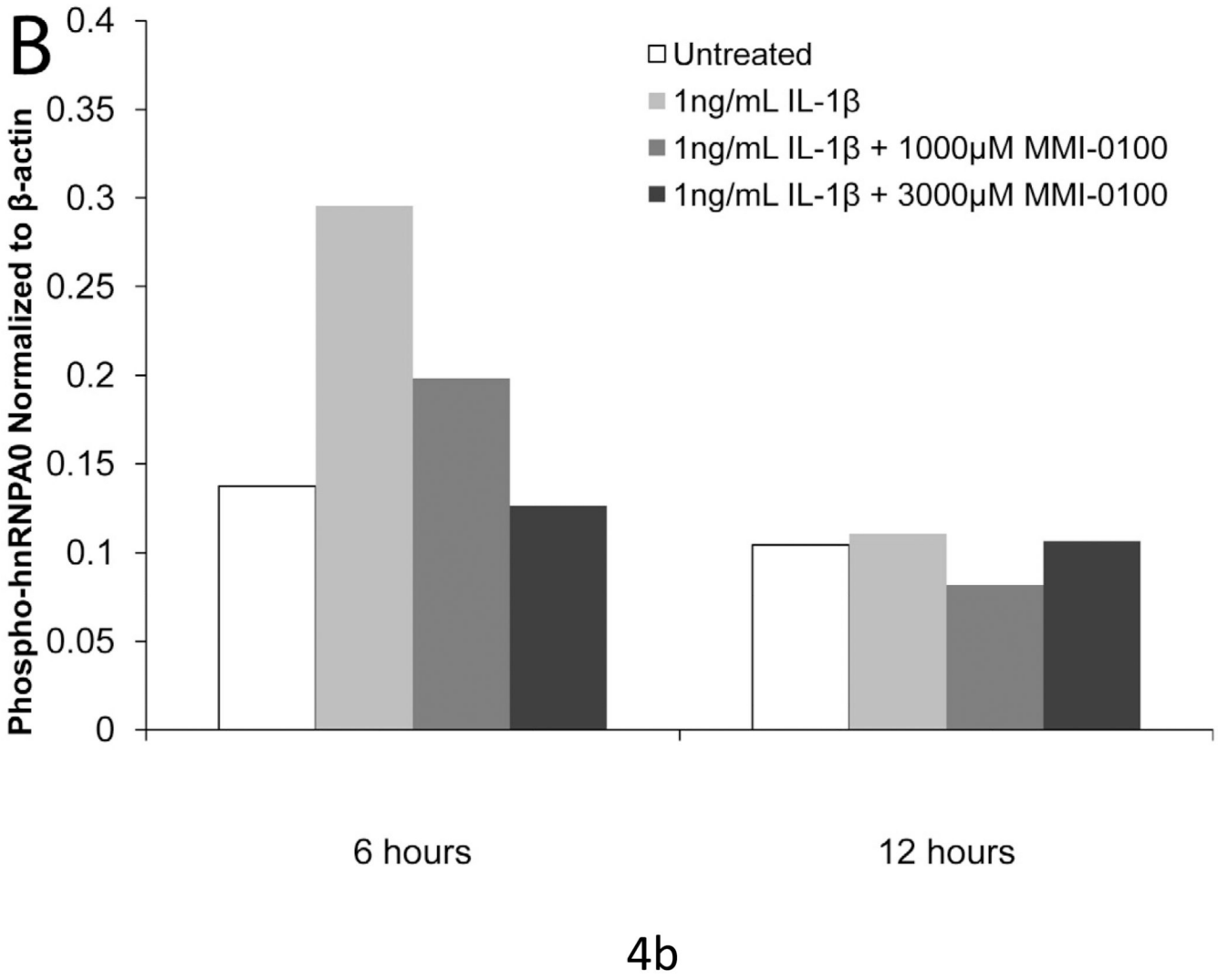

Figure 4. IL-1β induced phosphorylation of hnRNPA0 is reduced with MMI-0100 treatment

(A) Western blot and (B) densimetric analysis showing MMI-0100 reduces IL-1β induced phosphorylation of hnRNPA0 after 6 hours. IL-1β induced phosphorylation disappears at 12 hours: 1) untreated, 2) IL-1β, 3) MMI-0100 (1 mM), 4) MMI-0100 (3 mM)

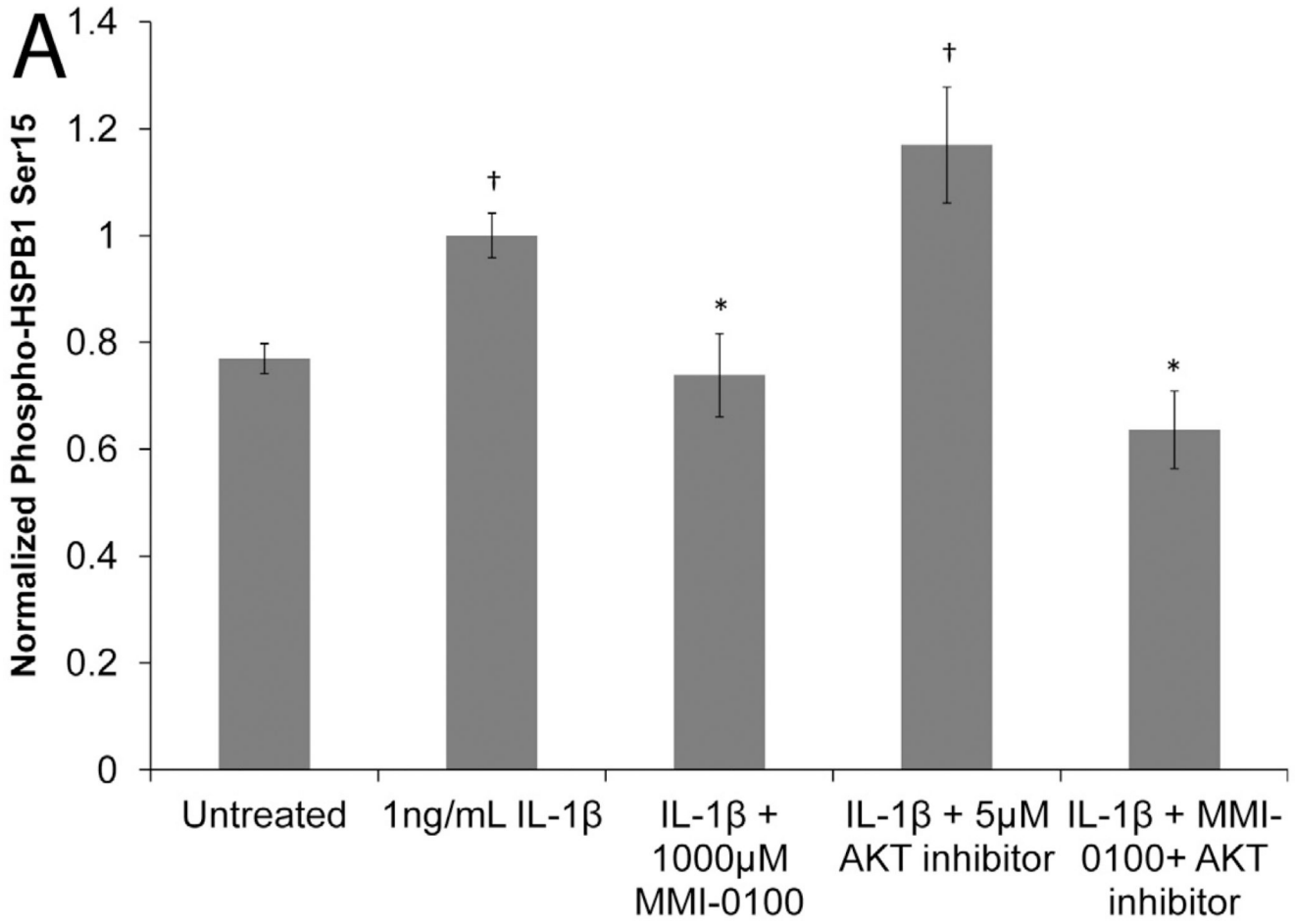

5a

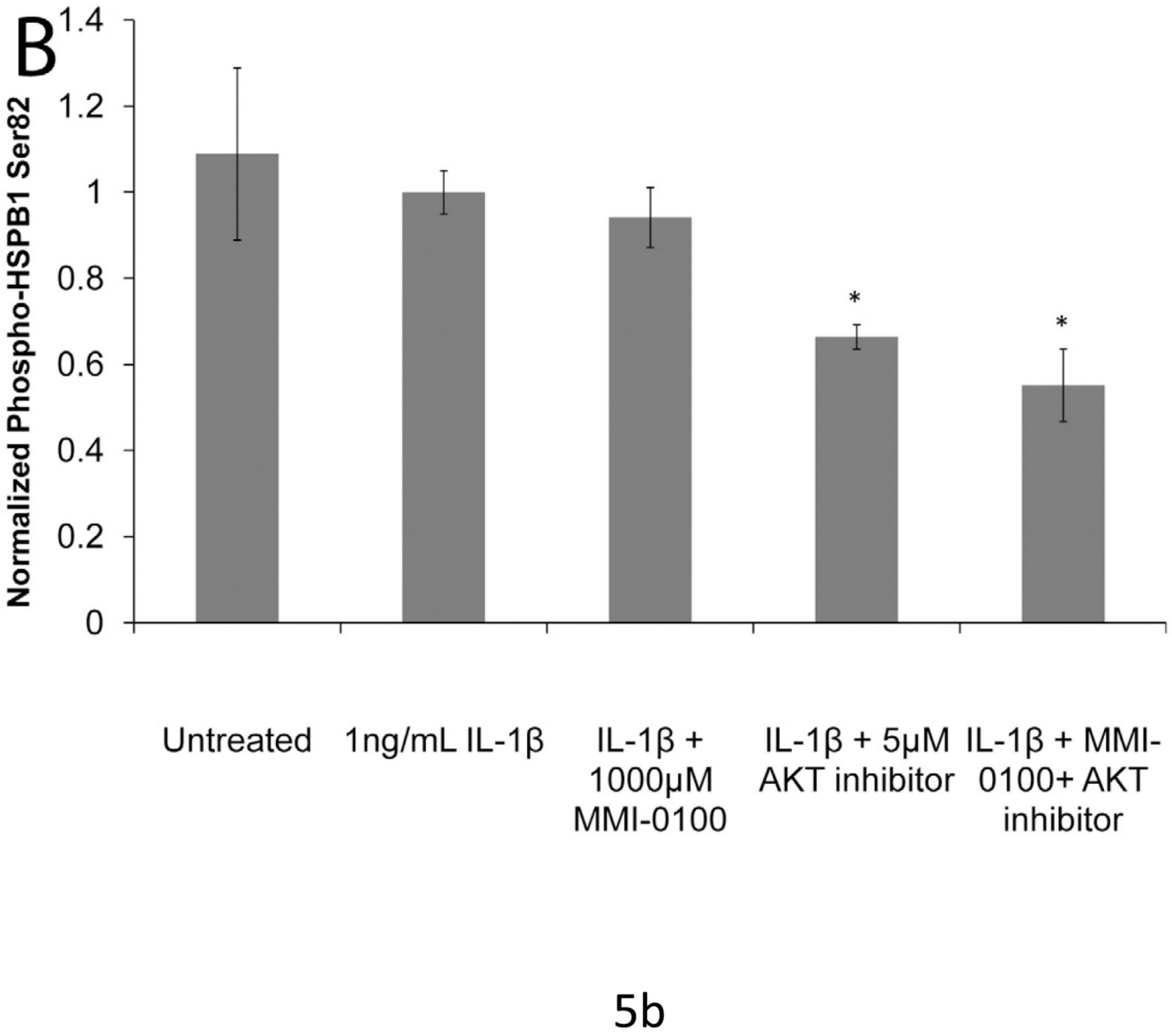

5b

Figure 5. IL-1β induced phosphorylation of HSPB1 with MMI -0100 treatment and AKT inhibition

(A) MMI-0100 treatment significantly decreases IL-1β induced HSPB1 phosphorylation at serine 15. (B) Treatment with an AKT inhibitor significantly reduced phosphorylation of HSPB1 at serine 82, which was not observed with peptide treatment. Data was normalized to total HSPB1 and cell number. Single factor ANOVAs were conducted with $p<0.05$. * = significantly lower than IL-1β treated. †=significantly higher than untreated. Error bars represent standard deviation between four samples.

Table 1

Adhesion scoring system.

Tissue adherent to anastomosis	**Score**
Abdominal wall	1
Colon	1
Epididymal fat	1
Omentum	1
Small bowel	1
Density	**Score**
Light, flimsy, easily dissected	1
Moderate, adherent, some force needed	2
Heavy, needs sharp dissection	3
Severe, not dissectable without damaging structures	4

Table 2

Summary of bowel anastomosis model results.

	Cumulative weight gain (g)	Bursting pressure (mmHg)	OHP anastomosis (absorbance)	Adhesion location score	Adhesion density score	Cumulative adhesion score
Control: 4 days	0.7±4.3	96±32	2679±475	2.2±0.2	2.4±0.2	4.7±0.4
Peptide: 4 days	−3.3±5.2	86±13	2055±184	2.0±0.2	2.1±0.2	4.1±0.3
p value	>0.05	>0.05	>0.05	>0.05	>0.05	>0.05
Control: 10 days	−5.6±3.1	191±29	4980±205	3.4±0.3	2.6±0.2	6.0±0.3
Peptide: 10 days	−1.3±3.7	175±27	5284±218	2.1±0.2	1.5±0.3	3.8±0.4
p value	>0.05	>0.05	>0.05	0.003	0.023	0.00296